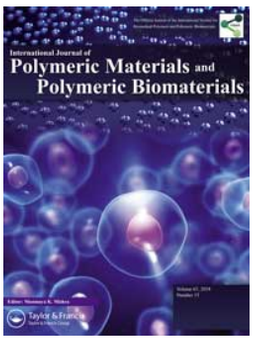

International Journal of Polymeric Materials and Polymeric Biomaterials

ISSN: 0091-4037 (Print) 1563-535X (Online) Journal homepage: https://www.tandfonline.com/loi/gpom20

Combined effects of 3D bone marrow stem cell-seeded wet-electrospun poly lactic acid scaffolds on full-thickness skin wound healing

Sadegh Ghorbani, Hossein Eyni, Taki Tiraihi, Leila Salari Asl, Masoud Soleimani, Amir Atashi, Shahram Pour Beiranvand & Majid Ebrahimi Warkiani

To cite this article: Sadegh Ghorbani, Hossein Eyni, Taki Tiraihi, Leila Salari Asl, Masoud Soleimani, Amir Atashi, Shahram Pour Beiranvand & Majid Ebrahimi Warkiani (2018) Combined effects of 3D bone marrow stem cell-seeded wet-electrospun poly lactic acid scaffolds on full-thickness skin wound healing, International Journal of Polymeric Materials and Polymeric Biomaterials, 67:15, 905-912, DOI: 10.1080/00914037.2017.1393681

To link to this article: https://doi.org/10.1080/00914037.2017.1393681

Accepted author version posted online: 20 Oct 2017.
Published online: 08 Jan 2018.

INTERNATIONAL JOURNAL OF POLYMERIC MATERIALS AND POLYMERIC BIOMATERIALS
2018, VOL. 67, NO. 15, 905–912
https://doi.org/10.1080/00914037.2017.1393681

Combined effects of 3D bone marrow stem cell-seeded wet-electrospun poly lactic acid scaffolds on full-thickness skin wound healing

Sadegh Ghorbani[a], Hossein Eyni[a], Taki Tiraihi[a], Leila Salari Asl[a], Masoud Soleimani[b], Amir Atashi[c], Shahram Pour Beiranvand[a] and Majid Ebrahimi Warkiani[d]

[a]Department of Anatomical Sciences, School of Medical Sciences, Tarbiat Modares University, Tehran, Iran; [b]Department of Hematology, School of Medical Sciences, Tarbiat Modares University, Tehran, Iran; [c]Stem Cell and Tissue Engineering Research Center, Shahroud University of Medical Sciences, Shahroud, Iran; [d]School of Mechanical and Manufacturing Engineering, Australian Centre for Nanomedicine, University of New South Wales, Sydney, Australia, Garvan Institute of Medical Research, Darlinghurst, Sydney, NSW, Australia

ABSTRACT

Tissue engineering has emerged as an alternative treatment to traditional grafts for skin wound healing. Three-dimensional nanofibers have been used extensively for this purpose due to their excellent biomedical-related properties. In this study, high porous 3D poly lactic acid nanofibrous scaffolds (PLA-S) were prepared by wet-electrospinning technique and seeded with rat bone-marrow stem cells (BMSCs) to characterize the biocompatibility and therapeutic efficacy of these fibers on the treating full-thickness dermal wounds. The results of *in vitro* and*in vivo* studies indicate that the 3D fibrous PLA-S can be a potential wound dressing for wound repair, particularly when seeded with BMSCs.

GRAPHICAL ABSTRACT

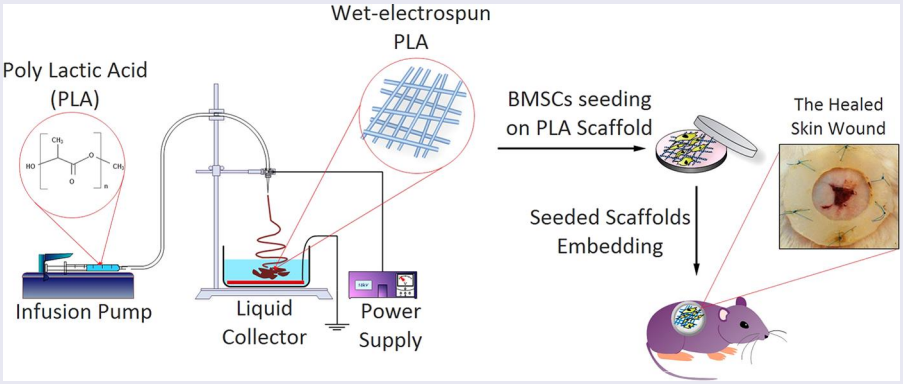

ARTICLE HISTORY
Received 28 June 2017
Accepted 20 October 2017

KEYWORDS
3D nanofiber scaffold; poly lactic acid scaffold; skin tissue engineering; wet electrospinning; wound healing

1. Introduction

Skin is the largest organ that provides a barrier against various damages to animal bodies.[1] Injuries to the skins occur by different physical or chemical agents. Wound healing is the process in which the cells can reconstruct and repair the injured tissue to reduce the size of the damaged or necrotic area.[2] Wound healing involves a set of events including inflammation surrounding the injured region, cellular migration and mitosis, angiogenesis and the expansion of the granulation tissue, extracellular matrix remodeling.[3] Cellular and biochemical components as well as enzymatic pathways play pivotal roles during the wound repair.[4]

Scaffold seeded with suitable cells is a feasible approach for wound repair and skin regeneration.[5] They are useful for treating deep wounds such as cutaneous burns. The interaction between various cell types and the scaffold is critical for angiogenesis, deposition of collagen and granulation tissue formation in wound healing.[6]

Nanofibers fabricated by electrospinning or other methods have attracted a significant interest over the last two decades owing to their porosity with excellent pores interconnectivity.[7,8] For example, nanofiber scaffolds closely mimic the natural extra cellular matrix that supports the cell attachment and proliferation.[9] moreover, those with small pore and a high surface to volume ratio can increase hemostasis without the use of a hemostatic agent resulting in wet environment for the wound by facilitating oxygen diffusion and allowing fluid repletion, effectively protect the wound from bacterial permeation. Consequently, nanofibers are promising materials to improve wound healing and skin regeneration.[10,11]

Until now, various polymeric biomaterials have been used in wound dressing applications.[12–14] The most common

CONTACT Taki Tiraihi takialtr@modares.ac.ir; ttiraihi@gmail.com Department of Anatomical Sciences, School of Medical Sciences, Tarbiat Modares University, P.O. Box 14155-4838, Tehran, Iran.
Color versions of one or more of the figures in the article can be found online at www.tandfonline.com/gpom.

natural biopolymer and synthetic polymers used as scaffold include alginate, collagen, gelatin, chitosan, polycaprolactone, poly (D,L-lactide-co-glycolide), polyvinyl alcohol, poly lactic acid (PLA), and others.[15] PLA is a Food and Drug Administration (FDA)-approved polymer well-known as a biocompatible and biodegradable polymer with good mechanical properties for tissue engineering application, such as bones repair, nerve, and skin tissue engineering, it is characterized by slow degradation rate in living tissue giving the damaged tissue enough time for repair.[16]

The major limitation of conventional electrospinning is that the scaffold produced has usually two-dimensional (2D) properties with limited pore density, which can obstruct cell infiltration near the superficial surface.[17]

Large specific surface area and high thickness of nanofibrous scaffolds lead to greater total surface area and consequently higher exudate absorption capacity.[18] Absorption of extra exudate is essential, because exudate accumulation under the dressing may lead to infection. Recently, a liquid collector (coagulation bath) was used to produce three-dimensional (3D) porous structures with high porosity and great control over the fiber thickness.[19,20] Wet-electrospun nanofibers have distinct advantages including their high porosity and surface area compared with dry electrospunning techniques.[21] However, one of the disadvantages of the electrospinning method is manufacturing 2D scaffolds.

In this study, we tried to use the wet electrospinning technique to produce the 3D biodegradable poly lactic acid scaffold (PLA-S) seeded with bone-marrow stem cell (BMSC) in treating skin wounds.

2. Experimental

2.1. Scaffold materials

Poly lactic acid with the average molecular weight (Mw) of 160,000 and the density of 1.25 g/cm^3 was obtained from Chemiekas GmbH (Germany), while the other solvents and experiment agents were purchased from Sigma-Aldrich (Steinheim, Germany). Dulbecco's modified Eagle's medium/Nutrient F-12 Ham (DMEM/F12) and fetal bovine serum (FBS) were purchased from Gibco (GIBCO-BRL, Eggenstein, Germany) while MTT (3-(4,5-dimethylthiazol-2-yl)-2,5-diphenyltetrazolium bromide) powder and dimethyl sulfoxide (DMSO) were purchased from Carl Roth (Karlsruhe, Germany).

2.2. Fabrication of wet-electrospun scaffold

Poly lactic acid with 15% concentration (w/v) was dissolved in chloroform in room temperature for 6 h. The solutions then were electrospun on aluminum collector and into the aqueous solution of sodium hydroxide (NaOH, pH 13) as coagulation bath. The electrospinning apparatus was consisted of a 10-mL syringe ended to an 18 gauge metal needle with a Teflon tube connecting to a positive high voltage source (HV100P OV, Fanavaran Nano-Meghyas, Iran), set to 18 kV. The syringe was placed into an infusion pump (Perfusor® compact S, B. Braun, Germany) with 3.8 mL/h infusion rate. The ejected solution was collected at room temperature on an aluminum foil grounded electrode connected to the high voltage supply and fixed on the floor of coagulation bath as a wet electrospinning. The depth of the bath was 5 cm while its surface was 10 cm beneath the needle tip. After electrospinning, they were removed from the coagulation bath then lyophilized at −77°C for 24 h (121550 PMMA, Christ, Spain).

2.3. Scaffold characterization

The morphology and cell attachment of the scaffold fibers was examined by scanning electron microscope (SEM) (SEM, AIS2100, Seron Technology, South Korea) as follows: the scaffolds were placed in six-well plates and seeded with BMSC for 3 days, washed with PBS and fixed for 30 min at room temperature with 2.5% glutaraldehyde. The scaffolds were then dehydrated by ethanol, dried overnight at room temperature, coated with gold for 180 s using a sputter coater (SC7620, Emitech, England) at 20 kV, and then examined under SEM. The average diameter of the nanofibers was statistically calculated using a computed image analyzer (ImageJ) by randomly measuring 20 different points. The diameters were presented as the average ± standard deviation.

The tensile strength was done on dry rectangular samples (10 × 30 mm) using a universal testing machine (Instron 5566: Canton, Massachusetts, USA) at a strain rate of 50 mm/min.

2.4. In vitro study

2.2.1. Isolation and characterization of BMSCs

Eight-week-old male Wistar rats were sacrificed by cervical dislocation, their femurs and tibiae were carefully cleaned from skin with pulling toward the foot, which was cut at the ankle bone. The ends of the tibia and femur were cut by sharp scissors. A 27-gauge needle was inserted and the marrow was aspirated with DMEM and collected in a 10-mL syringe. The bone marrow cells were cultured in DMEM containing 10% FBS, and penicillin–streptomycin–amphotericin B (100 U/mL, 100 µg/mL, and 0.25 µg/mL, respectively), cultured in T25 flask and incubated at 37°C with 5% CO_2. All animal experimental protocols were approved by the Institutional Animal Care and Use Committee of Tarbiat Modarres University (Tehran, Iran). The cell cultivation was performed up to the fourth passage. The cells were characterized using cell surface markers by fluorescence-activated cell sorting (FACS, Sysmex Partec CyFlow® Space) analysis. They were direct labeled with different cell markers with monoclonal antibodies CD45-FITC, CD14-PE, CD90-PE, CD44-FITC, and CD166-PE (eBioscience, USA San Diego). The differentiation potential of the BMSC was examined using cells harvested at the fourth passage. Adipogenic and osteogenic differentiations were performed according to the manufacturer's instructions in differentiated media (AdipoDiff Media and StemMACS™ osteoDiff Media: StemMACS™, Miltenyi Biotec GmbH, Germany). At day 21, the calcium mineralization was assessed by coloration with Alizarin Red stain (Sigma-Aldrich, San Diego, USA). For the adipogenic differentiation, the cells were confirmed following the standard protocols and analyzed by Oil red O staining after 14 days.

Finally, the BMSCs were seeded on wet-electrospun PLA-S (3D group) and on the same culture vessels without scaffolds as control (2D group).

2.2.2. Cell seeding on poly lactic acid nanofiber

The PLA-S nanofibers were cut into circular disks with 2 mm diameters. For scaffold sterilization, the samples were exposed to UV light for 2 h and then were immersed in 70% ethanol for 1 h and dried under vacuum for 1 h.[22] The scaffolds were washed twice with PBS and once with DMEM/F12, and were then transferred to a six-well plate under sterile condition while each was seeded with 7×10^4 cells, and incubated for 2 h in 4 mL cell culture medium with FBS.

2.2.3. Cells viability

The live/dead staining protocol using acridine orange (AO /ethidium bromide (EB) stains (AO/EB) was utilized for evaluating the viability of the cells at different conditions.[23] After incubating of 5000 BMSCs on scaffolds for 7 days, the medium on the wells was removed and 150 µL of AO/EB was added. Afterward, the cells were examined with a florescent microscope (TE 2000-S, Nikon, Tokyo, Japan). The cell proliferation was investigated by MTT assay after 1, 3, and 7 days of incubation. The formed purple formazan crystals were dissolved in DMSO. The absorption was read at 570 nm using Anthos 2020 microplate reader (Biochrom, Berlin, Germany).[24]

2.2.4. Cells attachment

The percentage of attached BMSCs on scaffolds was tested with the aid of MTT assay. The cells were seeded on the scaffolds and immediately transferred to an incubator and were incubated for 6 and 24 h. The samples then were washed twice with PBS for 30 s, and transferred to a new plate. The percentage of cell attachment was calculated using the mean absorbance value of the constructed specimen divided by that of negative control.[25]

2.3. In vivo study

The rats were randomly divided into three groups: a control group without any dressing (untreated group), treated with PLA-S (PLA-S group), and a treatment group where the PLA-S were seeded with BMSCs (PLA-S/BMSCs group).

2.3.1. Wound healing study

In an experimental study, 27 male Wistar rats (220 ± 20 g) of 2–3 months of age were chosen. General anesthesia was induced by intraperitoneal injection of mixture of Ketamine (Alfasan, Woerden, Holland; 0.04 mL/100 g body weight) and Xylazine (Alfasan, Woerden, Holland; 0.02 mL/10 g body weight). A 2 cm^2 circular full-thickness wound was done on the back skin of rats near neck posterior surface. After 7, 14, and 21 days, three rats from each group were sacrificed by cervical dislocation and full thickness skin samples (2.2×2.2 cm) were taken from the wound site and fixed in buffered formaldehyde (4%) for histological evaluations.

2.3.2. Evaluation of wound closure

On day 7, 14, and 21 of post-surgery, the dressing from the rats sacrificed was removed and several images were taken with a digital camera. The rate of wound closure was determined by the reduction in the wound size on digital image using the image J software (NIH, USA) ($n = 3$, for each group, on each time point). Finally, the wound site was excised, and the tissue was processed for histological evaluation.

2.3.2.1. Histology. The treated wound was immediately fixed with paraformaldehyde (4% in PBS, 0.01 M, and pH 7.4), and they were stained with hematoxylin and eosin (H&E), so as to evaluate the best stage of healing, and with Masson's Trichrome (MT) staining to study the extent of collagen deposition in the healed tissue during the period of wound healing. Images were taken with Axiophot microscope (Carl Zeiss GmbH, Germany).

2.3.2.2. Immunohistochemistry. Pancytokeratin AE1/AE3 antibody that recognizes a wide range of cytokeratins of different molecular weights. In the skin, AE1/AE3 tags the epidermis, the eccrine glands, and the folliculo-sebaceous-apocrine unit. Cytokeratin AE1 immunostains the basal layer of the epidermis, while cytokeratin AE3 immunostains the cytokeratins throughout the epidermis.

The tissue samples were embedded into paraffin, sectioned. The sections were deparaffinized, permeabilized with 0.1% Triton X-100 (Sigma-Aldrich) for 10 min and blocked in 3% (w/v) bovine serum albumin in PBS (pH 7.4) for 20 min at 20°C, incubated for 12 h at 4°C with mouse anti-rat pancytokeratin primary antibody (diluted 1:100) and washed with PBS (pH 7.4) (three times, each for 5 min). Subsequently, they were incubated for 30 min at 37°C with goat anti-mouse secondary antibody conjugated with FITC (diluted 1:300, Abcam, UK), washed with PBS (pH 7.4), counterstained with 4,6-diamidino-2-phenylindole stain and examined under a fluorescence microscope.

2.4. Statistical analysis

The results were statistically analyzed by SPSS (IBM SPSS Statistics, V.23, Armonk, New York) software using a one-way ANOVA test, the data were expressed as mean ± SE, $n \geq 3$. In all of the evaluations, $p < 0.05$ was considered statistically significant.

3. Results

3.1. Mechanical studies of scaffolds

The tensile of the wet-electrospun PLA-S is shown in Figure 1a. This scaffold had favorable mechanical properties for soft tissues such as the skin. The tensile strength of the dorsal skin from normal rats is about 1.2–3.2 MPa.[26] and this test illustrated that the tensile strength of wet-electrospun PLA-S is about 1.52 ± 0.15 MPa.

3.2. Characterization of scaffolds and cell-scaffold interactions

Scanning electron micrograph shows the morphology and average diameter of the nanofibers in PLA-S (2.74 ± 0.76 µm) and illustrate that the nanofibers were randomly oriented, forming a nonwoven porous structure (Figure 1b). The cell adhesion and spreading of the BMSCs was examined by SEM, which showed the cells attachment to the nanofibers

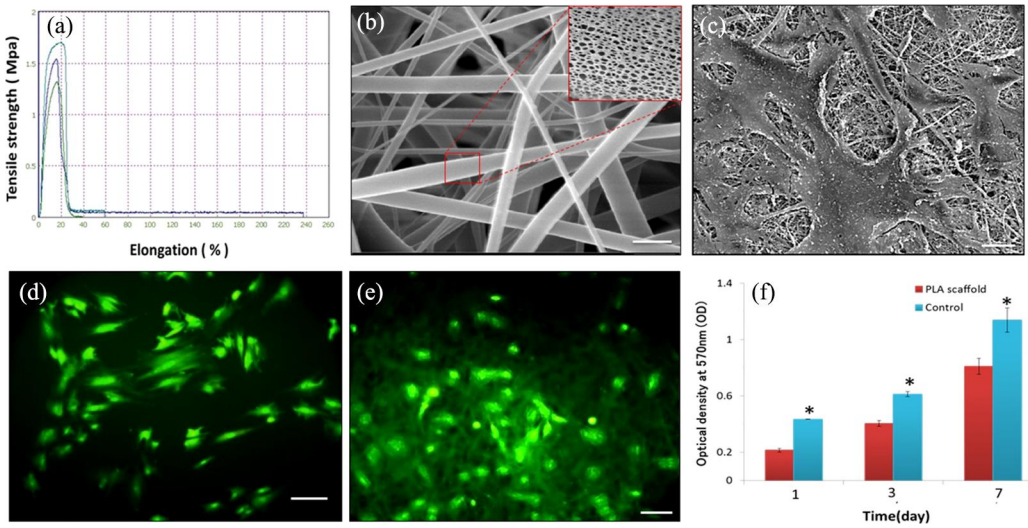

Figure 1. Mechanical, morphological and biological properties of the fabricated poly lactic acid scaffold (PLA-S). (a) the tensile strength of PLA-S (15%, w/v of PLA) (b) the scanning electron micrograph of fibrous PLA with nano-porous structures inside each fiber (inset: scale bar = 5 µm); scale bar = 5 µm. (c) the micrograph of the attached bone marrow stem cells on the PLA scaffold after 3 days; scale bar = 100 µm. (d and e) florescent micrographs of BMSCs in 2D (control) and 3D (PLA scaffold) substrates, respectively; scale bar = 100 µm (both). (f) MTT assay of the BMSCs in 2D and PLA-S (3D) at days 1, 3 and 7 (mean ± SE). *Statistically significant difference between the experimental and control groups ($P < 0.05$). *Note*: BMSCs, bone-marrow stem cells.

(Figure 1c). Also, the viability of cells was done by the live/dead technique using AO/EB staining in 2D and 3D cultures (Figure 1d, e, respectively), the later shows that the cells contacted and adhered to the scaffold.

3.3. In vitro *cells viability and attachment*

MTT assay was performed to evaluate the proliferation and attachment of the BMSCs on the PLA-S wet-electrospun scaffolds. The results were illustrated that the percentages of the cells adhered to scaffolds were 62 ± 1.73 and 76 ± 2.12% after 6 and 24 h, respectively. Regarding to results shown in Figure 1f, the cells proliferation on the PLA-S due to the hydrophobic nature of PLA nanofibers and lack of adequate surface reactive sites available for cellular interactions was lower than in the 2D control group.

3.4. *BMSCs characterization*

A selection of BMSCs markers was tested by flow cytometric analysis (Figure 2a to e). The cells were negative for CD45, CD14, while they were positive for CD90, CD44, and CD166 markers. The morphology of the BMSCs is presented in Figure 2f. The cells differentiated into osteogenic phenotype using osteogenic differentiation medium, and the results were confirmed with Alizarin red stain (Figure 2g). In addition, the adipogenic differentiation was done using adipogenic differentiation medium; the results were confirmed by the Oil O red stain (Figure 2h).

3.5. *PLA-S/BMSC effects on wound healing*

The effects of PLA-S and PLA-S/BMSCs on wound healing were evaluated in a rat full thickness excisional technique. The wound area was tracked over a period of 21 days, and the animals were sacrificed on days 7, 14, and 21 for histological analysis. On the 21st day post wounding (Figure 3a), the PLA-S/BMSCs group showed clear accelerated healing in comparison with that of the control group. Next to the PLA-S/BMSCs group, the PLA-S showed better healing than the untreated group. We found that the wound area of the PLA-S/BMSCs group is almost half of the PLA-S and one-third of the untreated ones. On the 21st day post wounding (Figure 3a), the PLA-S/BMSCs group showed nearly complete wound closure, whereas the PLA-S and the untreated groups recovered by about 75 and 50%, respectively. PLA-S showed equal potential of wound healing with BMSCs starting from day 7 post wounding. Furthermore, the high porosity of this scaffold promoted angiogenesis that caused the vessels run into the scaffold. This scaffold was embedded well in the wound area as the macroscopic view is presented in Figure 4d. According to the microscopic finding, the epithelialization process was significantly improved in the PLA-S/BMSCs group than the PLA-S alone and the untreated ones, implying that accelerated epidermal regeneration have an important role in the acceleration of wound closure under PLA-S nanofibers.

3.6. *Evaluation of wound closure*

The wounds had full-thickness were formed by circular 2 cm diameter excisions in the central region of the dorsal skin of the rat. The measurement of the wound area by digital imaging showed that the differences among the three groups were statistically significant on days 7, 14, and 21 after surgery (Figure 3b). These results clearly indicate that wound in the PLA-S/BMSCs group significantly improved as compared with the other groups.

3.7. *PLA-S/BMSCs effects on wound re-epithelialization and granulation tissue formation*

Skin sections were stained with H&E for general observation of skin layers and MT staining so as to evaluate the extent

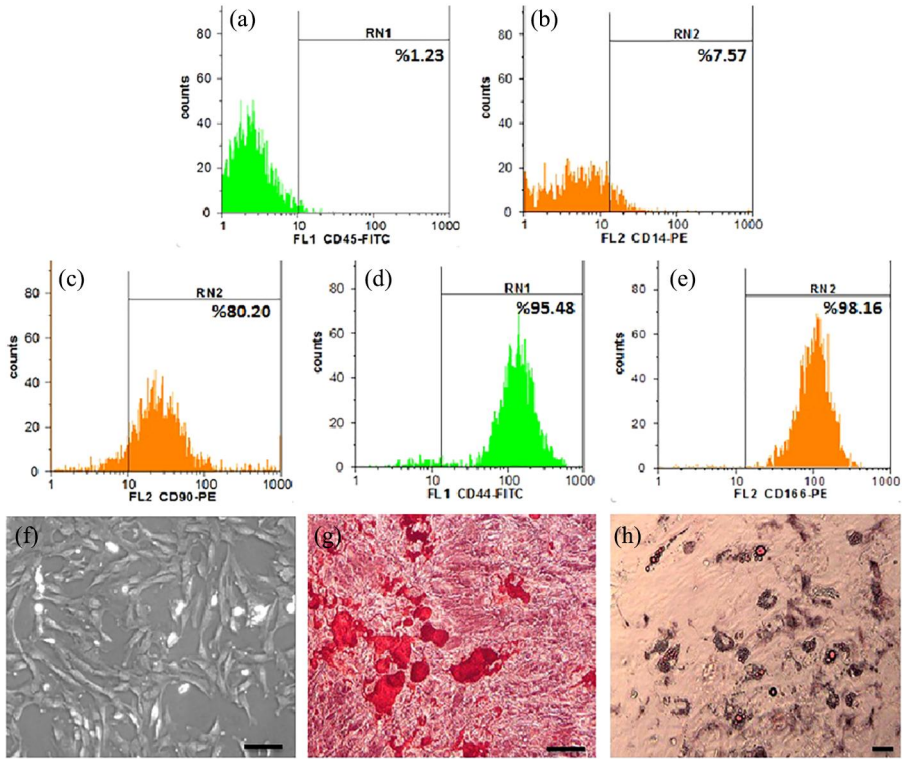

Figure 2. (a-e) characterization of BMSCs using flow cytometer, where BMSCs are labeled with monoclonal antibodies angainst CD45, CD14, CD90, CD44, and CD166, respectively. (f) a phase contrast image of the BMSC at passage 4. (g and h) represent the differentiation of the BMSC into osteogenic and adipogenic phenotypes; scale bar = 100 µm. *Note*: BMSCs, bone-marrow stem cells.

of collagen deposition in the healed tissue during the healing process. The histological results in the untreated, PLA-S only and PLA-S/BMSCs treated groups on the 7th, 14th, and 21st days of post-wounding are presented in Figure 4a, b. The PLA-S/BMSCs treated group showed significant healing response compared to the other groups. On day 7, in the untreated and PLA-S groups, the wounds were hypocellular with much thin epithelium, whereas in the PLA-S/BMSCs treated group, a moderate formation of thin epithelium was observed. However, it is worth to mention that in all of the groups the underlying dermis was not well organized. At the 14th day, the sections of the untreated group had a loose crust of dermal layers with poor epithelialization. The PLA-S and PLA-S/BMSCs treated groups showed a different degree of migration of the epithelium over the dermis, granulation tissue formation and dermal regeneration. On day 21, the PLA-S/BMSCs treated group showed re-epithelialization of the wound with well-formed and differentiated epithelium considerable increased deposition of connective tissue. Besides, the histological formation of capillaries containing blood could be seen easily in both groups of PLA-S and PLA-S/BMSCs in a newly formed skin tissue on 14th day (Figure 5a–d).

Masson trichrome (MT) stain showed the extent of compact collagen deposition at the healing area. Compared

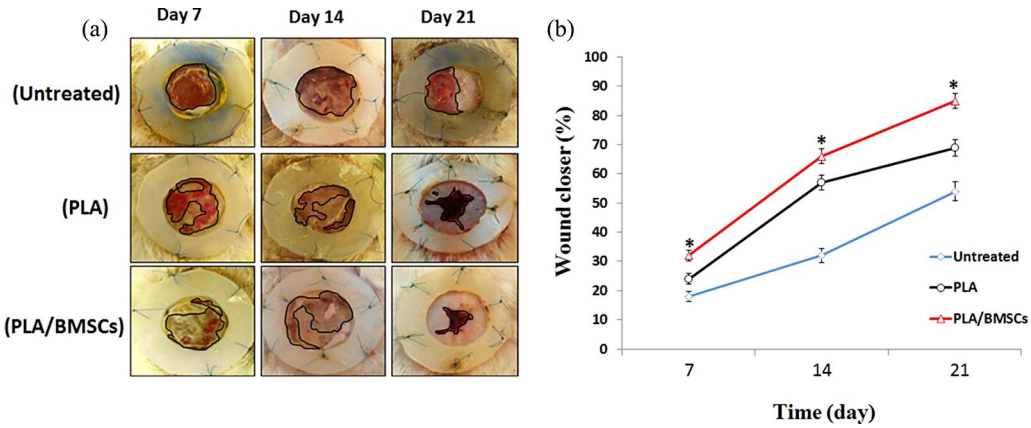

Figure 3. (a) the gross morphology of wound healing on the dorsum of rat at different time points (7, 14, and 21 days). The progressive healing of the wound is outlined by black lines. (b) the quantitative evaluation of the healing process using the percentage of wound closure at 7, 14, and 21 days of the experiment in untreated, PLA-S, PLA-S/BMSC groups. *Note*: PLA-S, poly lactic acid scaffolds; BMSCs, bone-marrow stem cells.

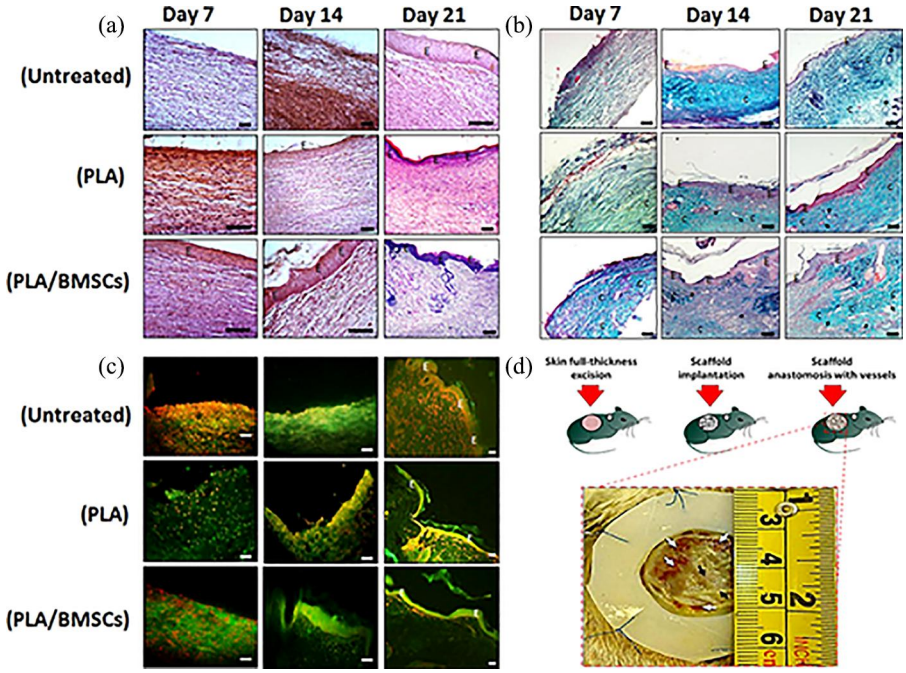

Figure 4. Histology of rat skin stained with hematoxylin and eosin, Masson's Trichrome (MT) stain, and immunohistochemistry (a, b, and c, respectively) of healing wounds collected from different groups (untreated, PLA-S, and PLA-S/BMSC); scale bar = 100 µm. (a and b) The layer of epidermis (e) and collagen fibers (c) in re-epithelialization processes sebaceous gland (S: red color). Also, many capillaries could be seen in the dermis of the PLA-S and the PLA-S/BMSC groups (black arrow) at day 14. (c) represents immunostaining with pancytokeratin raised against the skin layer of the healing tissue; scale bar = 100 µm. (d) Schematic images of the *in vivo* study that represent a macroscopic view of the healing process after 7 days in the PLA-S/ BMSC group. The black arrows indicate the scaffold embedded with the granulation tissues (white arrows). *Note*: PLA-S, poly lactic acid scaffolds; BMSCs, bone-marrow stem cells.

to the other groups, the PLA-S/BMSCs treatment resulted in higher collagen extent in the wounds obvious from the intensity of MT staining assay (Figure 4b). The untreated wound exhibited loose reticular arrangement of collagen, whereas in the case of PLA-S treated wounds, collagen was compact, dense, and well aligned. On day 21, a higher density

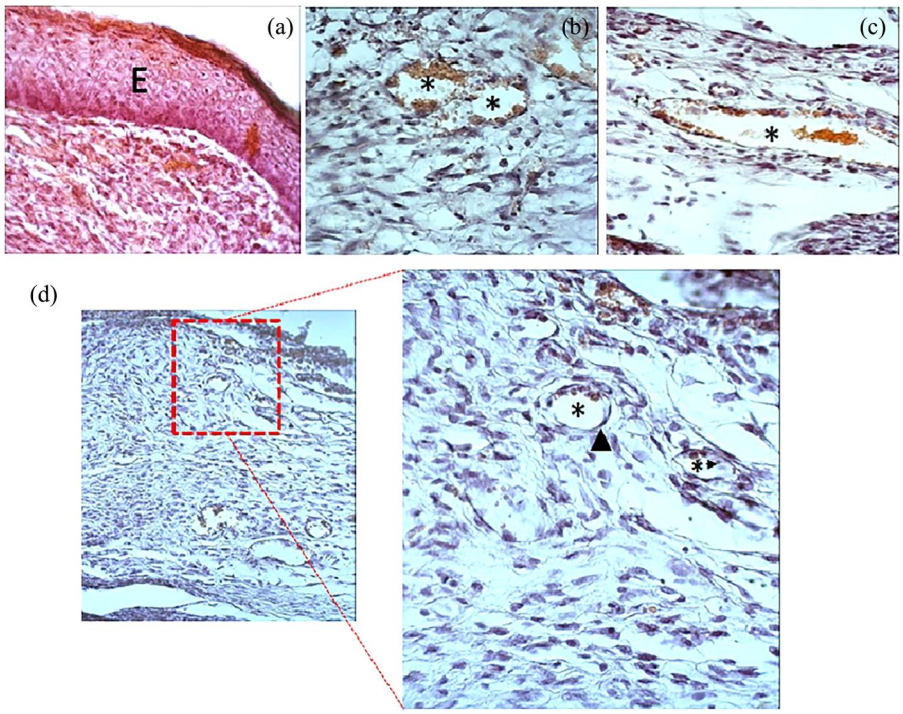

Figure 5. The histology of the healing skin from (PLA-S/BMSC) experimental group at day 14. (a) The full thickness of the epidermis with keratinization (E). (b) The cross section of capillaries (*) filled with blood in the granulation tissue while longitudinal capillary profile (*) is shown in (c). (d) The higher magnification of the granulation tissue containing capillaries (*) with flat thin endothelial cells (arrowhead), while the other capillary shows thicker immature endothelial cells with less red blood cells in the lumen. *Note*: PLA-S, poly lactic acid scaffolds; BMSCs, bone-marrow stem cells.

of collagen was observed in both the PLA-S and the PLA-S/BMSCs treated groups compared to the untreated one.

3.7. Cytokeratins immunoreactivity

On the 7th and 14th days, the cytokeratins were expressed on the basal layer of the epidermis. On the 21st day, cytokeratins were detected in the epidermis layers, but their expression was more significant in the PLA-S/BMSCs (Figure 4c).

4. Discussion

Recently, several studies have focused on designing wound dressings that can give rise and maintain an optimal wound healing environment. Nanofibrous dressings have been shown to accelerate wound healing.[11,27] In this study, a 3D PLA-S as a wound dressing has been fabricated using the wet-electrospinning technique as a novel method. The results from this study showed that the wet-electrospun PLA-S has three-dimensional and highly porous structure, which allows efficient gaseous exchange. It promotes wound healing by supplying oxygen, which is considered as an essential for energy provision, fibroblast proliferation, and collagen synthesis.[28,29]

The quasi-static tensile strength of the skin depends on Langer's line orientation.[30] In human body intagument, Langer's line often orient circumferentially, reinforcing current concepts of an intimate association between the microstructural organization of collagen and the mechanical properties of the skin, similar results have been documented in animals.[31] In general, circumferential orientation could stiffen the body at low strain compared with those longitudinally oriented. Tensile failure depends on the location, orientation, age and strain rate.[30] Therefore, the appropriate mechanical strength is very essential for skin substitutes (or wound dressings). In this study, the wet-electrospun PLA-S shows good tensile strength (1.52 ± 0.15 MPa) almost like that of the dorsal skin from rats (1.2–3.2 MPa).[26]

The interaction between electrospun PLA-S and stem cells such as human dermal fibroblasts, fibroblasts, endothelial, and somatic stem cells have been studied.[32–34] These *in vitro* studies showed that electrospun PLA-S supported stem cell proliferation and differentiation.[35,36]. In this study, the results of the MTT assay demonstrated that the viability trend of rat BMSCs on PLA-S was nearly similar to the 2D control group. This finding together with the well adherence and normal morphology for the BMSC on PLA-S nanofibers supports the hypothesis that the wet-electrospun PLA nanofibrous scaffold is biocompatible and promotes cell proliferation, however, such features of PLA can be improved by increasing the hydrophilic properties of this polymer. *In vivo* study of wet-electrospun PLA-S nanofibers as a wound dressing has not been reported before. It is likely that the matrices or scaffolds provided a platform for better attachment, proliferation, and differentiation of the cells. As such, the cells survived longer compared with sprayed and transplanted stem or somatic cells alone, which lacked a ready niche for homing in the hostile healing microenvironment containing inflammatory cells.[37]

Our *in vivo* results in the current study demonstrated that accelerate wound healing can be achieved by application of wet-electrospun PLA-S.[38] About $85 \pm 2.58\%$ wound closure was achieved on postoperative day 21 by PLA-S/BMSCs application compared to those without scaffold ($54 \pm 3.16\%$). The expression of cytokeratins is representative of a well-organized mature structure of newly formed dermis and epidermis under PLA-S dressing. Our comparison of the PLA-S with the PLA-S seeded by BMSCs revealed that PLA-S loaded with BMSCs can effectively accelerate wound closure of the wounds nearly higher than the pure PLA-S dressing in gross observation.

During normal wound healing, loose collagen fibers of early granulation tissues gradually are replaced by compact collagen fibers. Extensive depositions of thick compact collagen fibers on day 21 of the PLA-S/BMSCs group favor that of PLA-S nanofibers alone, which can effectively accelerate the improvement of dermal reconstruction. In this study, a new wound dressing based on 3D PLA nanofibers loaded by mesenchymal stem cells is introduced and shown to hold superior characteristics for the acceleration of wound healing. Although wet-electrospun PLA-S nanofibers were shown to have a noticeable superiority in the improvement of wound healing, there are several issues remained to be addressed including ease of use, patient acceptance and pain on removal which cannot be assessed in animal models.

The conclusion of the study is that a highly porous structure of PLA-S together with a high surface area of nanofibers allows appropriate gas exchange and exudate absorption. The *in vitro* and *in vivo* results of this study suggest that PLA-S alone and PLA-S seeded with bone-marrow derived mesenchymal stem cells are nontoxic and biocompatible. The results of 21 day treatment demonstrate that a source of BMSCs merging in nanofiber scaffolds as a wound dressing can promote skin wound healing.

5. Conclusion

The present study investigated the combined activity of PLA-S/BMSCs on wound healing. We demonstrated that PLA-S/BMSCs were capable to acceleration wound healing and significantly increased the wound closure by comprehensive healing which included cell proliferation and neo-epidermal thickness and improved tissue formation. These results suggest that PLA-S/BMSCs are promising particularly for the wound healing activity and may be possibly tested in the future in clinical study for the treatment of human skin wounds.

Acknowledgments

We are grateful for the support of the Faculty of Medical Sciences at Tarbiat Modares University, Tehran, Iran.

References

[1] Richardson, R.; Slanchev, K.; Kraus, C.; Knyphausen, P.; Eming, S.; Hammerschmidt, M. *J. Invest. Dermatol.* **2013**, *133*, 1655–1665.
[2] Pereira, R. F.; Barrias, C. C.; Granja, P. L.; Bartolo, P. J. *Nanomedicine* **2013**, *8*, 603–621.

[3] Akhundov, K.; Pietramaggiori, G.; Waselle, S. D.; Guerid, S.; Scaletta, C.; Hirt-Burri, N.; Applegate, L.; Raffoul, W. *Ann. Burns Fire Disasters* **2012**, *25*, 207.
[4] Mishra, P. J.; Mishra, P. J.; Banerjee, D. *World J. Stem Cells* **2012**, *4*, 35.
[5] Shevchenko, R. V.; James, S. L.; James, S. E. *J. R. Soc. Interface* **2009**, *7*, 229–258.
[6] Wojtowicz, A. M.; Oliveira, S.; Carlson, M. W.; Zawadzka, A.; Rousseau, C. F.; Baksh, D. *Wound Repair Regener.* **2014**, *22*, 246–255.
[7] Bhardwaj, N.; Kundu, S. C. *Biotechnol. Adv.* **2010**, *28*, 325–347.
[8] Wang, H.-S.; Fu, G.-D.; Li, X.-S. *Recent Pat. Nanotechnol.* **2009**, *3*, 21–31.
[9] Sill, T. J.; von Recum, H. A. *Biomaterials* **2008**, *29*, 1989–2006.
[10] Powell, H. M.; Supp, D. M.; Boyce, S. T. *Biomaterials* **2008**, *29*, 834–843.
[11] Choi, J. S.; Leong, K. W.; Yoo, H. S. *Biomaterials* **2008**, *29*, 587–596.
[12] Akturk, O.; Kismet, K.; Yasti, A. C.; Kuru, S.; Duymus, M. E.; Kaya, F.; Caydere, M.; Hucumenoglu, S.; Keskin, D. *J. Biomater. Appl.* **2016**, *31*, 283–301.
[13] Held, M.; Rahmanian-Schwarz, A.; Schiefer, J.; Rath, R.; Werner, J.-O.; Rahmanian, S.; Schaller, H.-E.; Petersen, W. *Dermatol. Surg.* **2016**, *42*, 751–756.
[14] Wang, S.; Yang, H.; Tang, Z.; Long, G.; Huang, W. *Stem Cells Int.* **2015**, *2016*, 1–8.
[15] O'brien, F. J. *Mater. Today.* **2011**, *14*, 88–95.
[16] Santoro, M.; Shah, S. R.; Walker, J. L.; Mikos, A. G. *Adv. Drug Delivery Rev.* **2016**, *107*, 206–212.
[17] Baker, S.; Sigley, J.; Helms, C. C.; Stitzel, J.; Berry, J.; Bonin, K.; Guthold, M. *Mater. Sci. Eng.* **2012**, *32*, 215–221.
[18] Babaeijandaghi, F.; Shabani, I.; Seyedjafari, E.; Naraghi, Z. S.; Vasei, M.; Haddadi-Asl, V.; Hesari, K. K.; Soleimani, M. *Tissue Eng. Part A.* **2010**, *16*, 3527–3536.
[19] Shin, T. J.; Park, S. Y.; Kim, H. J.; Lee, H. J.; Youk, J. H. *Biotechnol. Lett.* **2010**, *32*, 877–882.
[20] Ali, A. A.; Al-Asmari, A. K. *Appl. Nanosci.* **2012**, *2*, 55–61.
[21] Wang, X.; Min, M.; Liu, Z.; Yang, Y.; Zhou, Z.; Zhu, M.; Chen, Y.; Hsiao, B. S. *J. Membr. Sci.* **2011**, *379*, 191–199.
[22] Eyni, H.; Ghorbani, S.; Shirazi, R.; Salari Asl, L.; P Beiranvand, S.; Soleimani, M. *J. Biomater. Appl.* **2017**, *32*, 373–383.
[23] Raju, P. A.; McSloy, N.; Truong, N. K.; Kendall, M. A. *Vaccine* **2006**, *24*, 4644–4647.
[24] Kabiri, M.; Soleimani, M.; Shabani, I.; Futrega, K.; Ghaemi, N.; Ahvaz, H. H.; Elahi, E.; Doran, M. R. *Biotechnol. Lett.* **2012**, *34*, 1357–1365.
[25] Chen, L.; Bai, Y.; Liao, G.; Peng, E.; Wu, B.; Wang, Y.; Zeng, X.; Xie, X. *PLoS One* **2013**, *8*, e71265.
[26] Gallagher, A.; Ní Annaidh, A.; Bruyère, K. Dynamic tensile properties of human skin, (International Research Council on the 535 *Biomechanics of Injury*, **2012**, 494–501.
[27] Rho, K. S.; Jeong, L.; Lee, G.; Seo, B.-M.; Park, Y. J.; Hong, S.-D.; Roh, S.; Cho, J. J.; Park, W. H.; Min, B.-M. *Biomaterials* **2006**, *27*, 1452–1461.
[28] Gottrup, F. *World J. Surg.* **2004**, *28*, 312–315.
[29] Babior, B. M. *N. Engl. J. Med.* **1978**, *298*, 659–668.
[30] Haut, R. *J. Biomech. Eng.* **1989**, *111*, 136–140.
[31] Yamada, H.; Evans, F. G. *Strength of biological materials*, Ed., **1970**, 232–268.
[32] Doyle, V.; Pearson, R.; Lee, D.; Wolowacz, S.; Mc Taggart, S. *J. Mater. Sci. Mater. Med.* **1996**, *7*, 381–385.
[33] Hoveizi, E.; Nabiuni, M.; Parivar, K.; Rajabi-Zeleti, S.; Tavakol, S. *Cell Biol. Int.* **2014**, *38*, 41–49.
[34] Pavia, F. C.; La Carrubba, V.; Mannella, G. A.; Ghersi, G.; Brucato, V. *Chem. Eng. Trans.* **2012**, 27–31.
[35] Kumbar, S. G.; Nukavarapu, S. P.; James, R.; Nair, L. S.; Laurencin, C. T. *Biomaterials* **2008**, *29*, 4100–4107.
[36] Shabani, I.; Haddadi-Asl, V.; Seyedjafari, E.; Babaeijandaghi, F.; Soleimani, M. *Biochem. Biophys. Res. Commun.* **2009**, *382*, 129–133.
[37] Zhong, S.; Zhang, Y.; Lim, C. *Wiley Interdiscip. Rev. Nanomed. Nanobiotechnol.* **2010**, *2*, 510–525.
[38] Hermans, M. H. *J. Burn Care Res.* **2007**, *28*, 835–847.